

SMALL-ANGLE X-RAY STUDY OF DNA-DEPENDENT RNA POLYMERASE SUBUNIT σ FROM *ESCHERICHIA COLI*

Otto MEISENBERGER, Ingrid PILZ* and Hermann HEUMANN[†]

*Institut für Physikalische Chemie der Universität Graz, Heinrichstr. 28, A-8010 Graz, *Institut für Physikalische Chemie der Universität Graz, Heinrichstraße 28, A-8010 Graz, Austria and [†]Max-Planck-Institut für Biochemie, 8033 Martinsried bei München, FRG*

Received 30 November 1979

1. Introduction

The σ subunit of RNA polymerase of *Escherichia coli* stimulates specific initiation of transcription [1,2]. After the synthesis of a RNA chain of ~ 10 nucleotides [3] the σ factor dissociates from the ternary complex consisting of RNA polymerase (core enzyme), DNA and RNA, and can be reused as initiation factor. For the understanding of the function of the σ factor it is necessary to know its structure, isolated as well as in the complex with core enzyme. Here the structure of isolated σ subunit (mol. wt 92 000) is investigated by small angle X-ray scattering.

2. Materials and methods

2.1. Preparation of σ subunit

The σ subunit was prepared from RNA polymerase as in [3]. RNA polymerase was isolated from *E. coli* by the procedure in [4] with slight modifications: TAG buffer (not containing $MgCl_2$) was used instead of TMAG. The bulk of proteins was eluted with TAG containing 0.55 M instead of 0.6 M NH_4Cl . Only one zonal centrifugation was performed at high salt.

For elimination of unspecific aggregate σ subunit was sedimentated in a sucrose–glycerol gradient. The main fractions were pooled, concentrated by ammonium sulfate precipitation and dialysed overnight against a buffer containing 0.05 M Tris–HCl (pH 7.5), 0.55 M NH_4Cl and 10^{-3} M 2-mercaptoethanol. This σ fraction stimulated transcription of core enzyme on T7 DNA by a factor of 10.

The purity of the σ factor was $>95\%$ as checked by SDS gel electrophoresis. The homodispersity of σ was checked by sedimentation in an ultracentrifuge (Spinco model E). The σ factor has run as single sedimentating material. The $[\sigma \text{ factor}]$ was determined by means of the staining procedure [5], which was calibrated as in [6].

2.2. Small-angle X-ray scattering

The measurements were carried out with a Kratky camera with slit collimation system [7] on a X-ray generator with a copper tube (50 kV, 30 mA).

Enzyme solutions were investigated at 4°C. Scattered intensities were recorded at 96 different angles over 0.00216–0.123 radians, using an entrance slit of 120 μm .

The detection system consisted of a proportional counter with pulse-height discriminator, tuned to the $Cu K_\alpha$ line. The contribution of the K_β line was determined as in [8]; the appropriate correction was applied in the course of the desmearing procedure with the indirect transformation method [9].

Each scattering curve was recorded several times with a fixed number (10^5) of pulses per angle in order to minimize statistical errors. The preliminary data reduction was performed with a computer program from [10]. Methods and procedures used for calculation of volume and radius of gyration are in [11,12].

3. Results and discussion

3.1. Radius of gyration and maximum dimension

A concentration series was measured over 5–8 mg/ml. The inner parts of the scattering curves were

* To whom correspondence should be sent

plotted according to Guinier ($\log I/c$ vs $(2\theta)^2$) and extrapolated to zero concentration. This plot should yield a straight line whose slope is proportional to the square of the radius of gyration. After desmearing the radius of gyration was calculated to be $R = 4.2 \pm 0.1$ nm. This value agrees with the value computed from the $p(r)$ function according to:

$$R^2 = \frac{\int_0^\infty p(r) r^2 dr}{2 \int_0^\infty p(r) dr}$$

The intraparticle distance distribution function $p(r)$ was calculated with the evaluation program [9]. $p(r)$ becomes zero at values of r exceeding the maximum particle dimension D_{\max} . Thus determined, D_{\max} amounts to 14.6 ± 0.5 nm. The $p(r)$ function of factor σ is shown in fig.1 the desmeared scattering curve in fig.2.

3.2. Volume

The volume of a hydrated macromolecule is proportional to its scattered intensity at zero angle and inversely proportional to its invariant Q [13].

Q was determined from a plot $I(2\theta)^2$ vs (2θ) by numerical integration (Simpson) between $2\theta = 0$ and 0.05 radians and by analytical integration for the tail end ($k/(2\theta)^4$). The volume of factor σ was found to

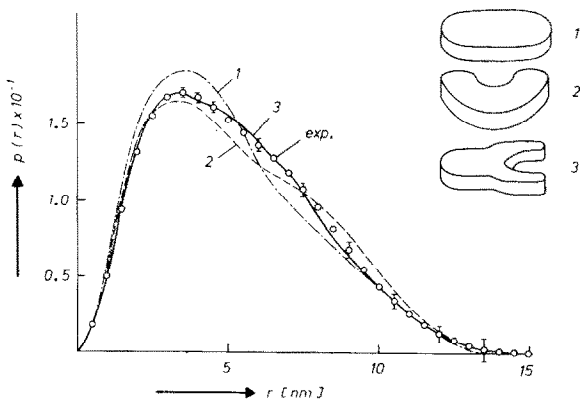


Fig.1. Comparison of the experimental distance distribution function $p(r)$ of factor σ (○—○—○) with the theoretical one of model 1 (---), model 2 (- · -) and model 3 (—). r = distance; Φ = experimental data including propagated standard deviation. The deviation of the theoretical curve of model 3 from the experimental one does not exceed the error band of the latter.

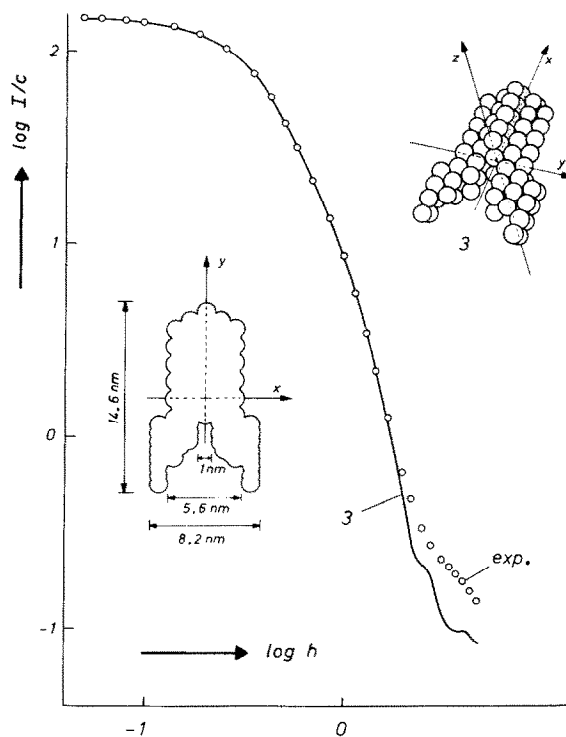


Fig.2. Comparison of the experimental scattering curve of factor σ (○—○—○) with the theoretical one of model 3 (—). I = scattered intensity; c = concentration; $h = (4\pi/\lambda) \sin \theta$ (λ = wavelength of the Cu K α line, 2θ = scattering angle). Perspective and top view of model 3. In model 3 the thickness of 2.4 nm of the disk-shaped particle was approximated by 2 layers of spheres.

be $136 \text{ nm}^3 \pm 5\%$ by this method. Experience shows that the volume calculated from the invariant is usually affected by errors of $\geq 5\%$, presumably due to particle inhomogeneities which come into effect at large angles.

3.3. Shape

Small-angle X-ray scattering allows the direct determination of several parameters, such as, radius of gyration, maximum dimension and volume. The particle shape on the other hand can only be determined indirectly; the most common technique is to make a plausible assumption of the particle shape and compare the theoretical scattering curve or the intraparticle distance distribution $p(r)$ with the experimental curves. The comparison is usually more convenient in real space ($p(r)$) than in reciprocal space ($I(2\theta)$) [14].

Test-calculations of a large number of possible

particle structures were performed to exclude models which do not agree with the experimental observations. Proceeding this way a model was found fitting well the experimental scattering curve. Since another model with the same number of parameters could not be found, this model is reasonable. It should, however, be emphasised that further models may exist that fit the experimental curve sufficiently well.

All model calculations were carried out with a computer program which uses Deye's formula [15] to calculate the theoretical scattering curves of models composed of spherical subunits:

$$I(h) = \sum_{k,i=1}^n G_i \Phi_i(h) G_k \Phi_k(h) \frac{\sin(d_{ik}h)}{d_{ik}h}$$

where $I(h)$ = scattered intensity, $h = (4\pi/\lambda) \sin \theta$ (λ = wavelength of the Cu K_α line, 2θ scattering angle), $G_i = g_i r_i^3$ (g_i , weighting factor for the electron density; r_i , radius of the subunit i); d_{ik} = distance between the subunit i and k ; $\Phi_i(h)$ = form factor for spherical subunits:

$$\Phi_i(h) = \frac{3 \sin(hr_i) - hr_i \cos(hr_i)}{(hr_i)^3}$$

Since the distance distribution function $p(r)$ from σ (fig.1) shows that the particle must have a rather anisotropic structure, the indirect Fourier transform was used to calculate the distance distribution functions of the cross-section $p_c(r)$ and of the thickness $\lambda_T(r)$. Both operations were carried out with computer programs [16]. The $p_c(r)$ function shows an anisotropic cross-section of σ , the $\lambda_T(r)$ function decreases linearly and becomes zero at 2.4 nm, which corresponds to the thickness of the particle.

The comparison of the experimental scattering curves of σ with the theoretical scattering curves of simple triaxial bodies (taking into account also the experimental data mentioned, radius of gyration, thickness and volume) led to the first model, an elongated disc with the dimensions $a:b:c = 7.2 \text{ nm} : 3.4 \text{ nm} : 1.2 \text{ nm}$ (model 1, fig.1). Its distance distribution function shows that the structure is too compact (lack of distances between 6 and 9 nm).

To take these discrepancies into account, models of increasing complexity like kidney shaped, bended and L-shaped models were calculated. Model 2 in fig.1

shows one of those structures, which, however were in unsatisfactory agreement.

Finally, a y-shaped model was found to fit the experimental scattering curve fig.2 and the $p(r)$ function best (fig.1, model 3). It consists of 93 spheres with a radius of 0.7 nm (fig.2). The thickness of 2.4 nm corresponds to 2 layers of spheres.

Further model calculations of the subunit α_2 , of the partial complex $\beta\alpha_2$, and of RNA polymerase core enzyme and holoenzyme are in progress.

Acknowledgements

I.P. and O.M. thank the Österreichischen Fonds zur Förderung der wissenschaftlichen Forschung for generous support. Our thanks are also due to the Verein Österreichischer Chemiker for the scholarship from the Herman F. Mark Forschungsförderungs Fonds. We also thank B. Müller for drawing the figures. H.H. thanks the Deutsche Forschungsgemeinschaft for generous support of this work, Peter Stöckel for valuable discussion and Gisela Buer for excellent technical assistance.

References

- [1] Burgess, R. (1966) J. Biol. Chem. 244, 6168.
- [2] Burgess, R., Travers, A. A., Dunn, J. J. and Bautz, E. K. F. (1969) Nature 221, 43.
- [3] Burgess, R. R. and Travers, A. A. (1971) Methods Enzymol. 21D, 500.
- [4] Zillig, W., Zechel, K. and Halbwachs, H. J. (1970) Hoppe Seylers Z. Phys. Chem. 351, 221–227.
- [5] Heil, A. and Zillig, W. (1970) FEBS Lett. 11, 165–172.
- [6] Heumann, H., Stöckel, P. and May, R. (1980) in preparation.
- [7] Kratky, O. (1958) Z. Elektrochem. 62, 66–73.
- [8] Zipper, P. (1969) Acta Phys. Austriaca 30, 143–151.
- [9] Glatter, O. (1977) J. Appl. Crystallogr. 10, 415–421.
- [10] Zipper, P. (1972) Acta Phys. Austriaca 36, 27–38.
- [11] Kratky, O. (1963) Prog. Biophys. 13, 105–173.
- [12] Pilz, I. (1973) in: Physical Principles and Techniques of Protein Chemistry (Leach, S. J. ed) part C, pp. 141–243, Academic Press, New York.
- [13] Porod, G. (1951) Kolloid Z. 124, 83–114.
- [14] Glatter, O. (1979) J. Appl. Cryst. 12, 166–175.
- [15] Glatter, O. (1972) Acta Phys. Austriaca 36, 307–315.
- [16] Glatter, O. (1980) in preparation.